

UDC 654.165

doi:10.15217/issn1684-8853.2015.1.68

## DEPOLARIZATION EFFECTS OF RADIO WAVE PROPAGATION IN VARIOUS LAND BUILT-UP ENVIRONMENTS

**Y. Ben-Shimol**<sup>a</sup>, PhD, Electrical Engineering, Senior Lecturer, benshimo@bgu.ac.il

**N. Blaunstein**<sup>a</sup>, Dr. Sc., Phys.-Math., Professor, nathan.blaunstein@hotmail.com

**M. B. Sergeev**<sup>b</sup>, Dr. Sc., Tech., Professor, mbse@mail.ru

<sup>a</sup>Ben-Gurion University of the Negev, POB 653, 1, Ben Gurion St., Beer Sheva, 74105, Israel

<sup>b</sup>Saint-Petersburg State University of Aerospace Instrumentation, 67, B. Morskaja St., 190000, Saint-Petersburg, Russian Federation

**Purpose:** A detailed analysis of the spatial-temporal variations of the polarized characteristics of an elliptically polarized radio wave propagating in various built-up environments. **Methods:** Analysis of the classical methods used for defining the polarized parameters of homogeneous monochromatic plane waves, arriving at the receiver antenna from various directions in free space, is briefly presented. These methods are adapted for the propagation scenarios occurring in four land built-up environments, where the complicated stochastic variations of wave polarization parameters have been observed experimentally and when the canonical methods are ineffective. The 3D classical presentation of the geometrical parameters of the polarized ellipse and Stocks parameters are used to analyze the co-polarized and cross-polarized components of the wave intensity in the vertical and horizontal plane of the polarization ellipse and their relations with the main parameters and characteristics of the built-up terrain are explored. **Practical Relevance:** The presented analysis allows to estimate theoretically the angle of wave depolarization and the polarization loss effects in rural, mixed residential, sub-urban, and urban areas. Such estimation allows designers of cellular networks to predict reception problems due to de-polarization in the presence of stochastic disturbances. Measurements that are taken prior to the deployment of cellular networks can now be limited to "problematic antenna positions" that are predicted by the presented model. To the best knowledge of the authors such results are presented for the first time.

**Keywords** – Depolarization, Propagation Channels, Built-up Environments.

### Introduction

During propagation in the space domain, all radio waves can be decomposed into two wave components mutually orthogonal in the plane perpendicular to the direction of propagation. A complete description of the polarization state of a radio wave under consideration consists of the magnitude of its mutually orthogonal electrical field components that may differ in magnitude and phase, determining the type of wave polarization: linear, circular or elliptical, (see [1–8] and bibliography therein). One of the main problems (among other complicated problems), observed in the recent 4–5 decades, was the effect of the polarization discrimination or mismatch (called the depolarization) occurring in the land communication channels: rural, mixed residential, sub-urban and urban [9–18]. As was shown by numerous measurements and experiments carried in different terrestrial built-up environments, the effects of depolarization are caused by multipath phenomena due to multiple reflection, diffraction and scattering from natural and artificial obstructions located in areas of service surrounding the transmitter and the receiver antennas [19–26]. To mitigate and overcome these effects from the beginning, several methods were proposed, based on usage of the polarization diversity techniques [14–18, 27–29] or the use of adaptive (smart) nar-

row-beam antennas with elliptical-like polarization [8, 30, 31], instead of those having vertical and/or horizontal polarization [14–18, 27–29]. In further investigations in elliptically polarized antennas, the effects of rotation of the polarization ellipse on the angle called depolarization angle, show changes its shape and in the ratio of its main axes, a redistribution of wave energy along the elliptic axes, and finally, loss of the wave field energy. The classical theoretical frameworks and experimental techniques, performed during the sixties to nineties period of the last century, have drawn the attention to the definition of the polarized parameters of homogeneous monochromatic plane waves arriving at the receiver antenna from various directions in free space, mostly on the geometrical parameters of the polarized ellipse and on Stocks parameters [3, 9–13]. These approaches were usually related to the tasks of selecting and remote sensing of different targets in radio-location based on data concerning kinds of polarization of the reflected signal from targets. Another use was obtaining a stable wireless communication in various land environments. Thus, these methods were adapted to the problems of wireless communications focusing the attention on the analysis of complicated interference fields, formed in conditions of multipath propagation of radio waves in the land built-up environment, where the canonical methods become ineffective.

This happens, since the parameters of the polarized ellipse and its spatial orientation become to be the local characteristics of the field in such multiray built-up channels, which are significantly changed with distance defined by the characteristic scale of interference variations of the field amplitude or intensity [27–31]. Based on a classical presentation of the geometrical parameters of the polarized ellipse and on Stocks parameters, the co-polarized and cross-polarized components of the signal intensity variations in the vertical and horizontal plane of the polarization ellipse were obtained. Unfortunately, a close relation between the parameters of depolarization, such as the angle of depolarization and the depolarization losses, and different “responses” of the various land environments, rural, sub-urban and urban, on radio propagation was lacking. The development of the unified stochastic approach during the nineties of the last century [13–18, 27, 28], provided a detailed description of the relations of the main parameters of the built-up terrain and its features with radio wave intensity variations in the space, angle-of-arrival and time-of-arrival domains. The unified stochastic approach enables to investigate the effects of depolarization on elliptically polarized radio wave propagating through various land channels – rural, mixed residential, sub-urban and urban became possible. As was shown in [3, 8–13, 28–30]..., in a land built-up environment, the direction of the normal vector to the plane of the polarized ellipse cannot be related to the desired direction of any wave propagation, and its changes have stochastic character depending on the amount of waves, arriving at the observation point, their direction of arrival, amplitude and phase variations.

**Main Characteristics and Vectors of the Polarized Ellipse**

Let us consider a spatial coordinate system determined by a set of three orthogonal unit vectors  $\{\mathbf{u}_1 \equiv \mathbf{x}, \mathbf{u}_2 \equiv \mathbf{y}, \mathbf{u}_3 \equiv \mathbf{z}\}$  (for unification in our further derivations the results obtained in [3, 10–15]). In this general case, any vector of the electric field can be determined by three components [3, 9–13]:

$$E(t) = \mathbf{u}_i E_i(t) = \mathbf{u}_i A_i \cos(\omega t + \psi_i), \quad i = 1, 2, 3, \quad (1)$$

where  $A_i$  and  $\psi_i$  are the amplitude and phase of the component with number  $i$ ;  $t$  is the current time;  $\omega$  is the angular frequency,  $\omega = 2\pi f$ . The well-known components of the total field, called the sine and the cosine components of the total field are defined as [3, 10–13]

$$S_i = -A_i \sin \psi_i, \quad C_i = A_i \cos \psi_i. \quad (2)$$

These components perform two three-dimensional (3D) vectors, respectively:  $\mathbf{S}(S_1, S_2, S_3)$  and

$\mathbf{C}(C_1, C_2, C_3)$ . In such definitions, we can rewrite (eq:1) as

$$\mathbf{E}(t) = \mathbf{S} \sin \omega t + \mathbf{C} \cos \omega t. \quad (3)$$

The large and the small semi-axis of the ellipse can be determined by the extremes of  $\mathbf{E}(t)$ . In [3, 10–13] it was shown that

$$|\mathbf{E}(t)|^2 = \frac{S^2 + C^2}{2} + \cos(2\omega t) \left[ \frac{C^2 - S^2}{2} + \mathbf{CS} \tan(2\omega t) \right]. \quad (4)$$

The extremes of  $|\mathbf{E}(t)|^2$ , which defines each semi-axis of the ellipse, can be presented as

$$|\mathbf{E}_{\min}|^2 = \frac{S^2 + C^2}{2} - \left[ \left( \frac{C^2 - S^2}{2} \right) + (\mathbf{CS})^2 \right]^{1/2};$$

$$|\mathbf{E}_{\max}|^2 = \frac{S^2 + C^2}{2} + \left[ \left( \frac{C^2 - S^2}{2} \right) + (\mathbf{CS})^2 \right]^{1/2}. \quad (5)$$

Using expression (2) we can relate all six projections of the vectors  $\mathbf{C}$  and  $\mathbf{S}$  with three amplitudes  $A_i$  and three phases  $\psi_i, i = 1, 2, 3$ , of the total field. Unfortunately, in practice, the components of the vectors  $\mathbf{C}$  and  $\mathbf{S}$  cannot be measured directly; they usually relate to the Stocks parameters, which can be easily measured.

We now introduce the polar angles,  $\varphi \in [0, 2\pi]$  and  $\theta \in [0, 2\pi]$ , fixing the position of the normal  $\mathbf{N}$  with respect to coordinate axes:

$$\varphi = \tan^{-1} \frac{N_2}{N_1}; \quad \theta = \tan^{-1} \frac{N_3}{N_1}. \quad (6)$$

Finally, we can obtain the components  $C_i$  and  $S_i$  that allow us to calculate the total intensity of the field:

$$I = \sum_{i=1}^3 A_i^2 = C^2 + S^2. \quad (7)$$

Accounting now for (2) and (7), we get from (5) the following expressions of the semi-axes of the ellipse

$$E_{\max} = \left\{ \frac{I}{2} + \left[ \left( \frac{I}{2} \right)^2 - N^2 \right]^{1/2} \right\}^{1/2};$$

$$E_{\min} = \left\{ \frac{I}{2} - \left[ \left( \frac{I}{2} \right)^2 - N^2 \right]^{1/2} \right\}^{1/2}. \quad (8)$$

We also obtain the *elliptical coefficient*, which is equal to the ratio of the small and large semi-axes, that is,

$$R = \frac{2N}{I + \left( I^2 - 4N^2 \right)^{1/2}}. \quad (9)$$

At the same time, in [3, 9–13] it was shown that Stocks coefficients can be usually used for these purposes. Therefore, following [3, 9–13], we present these parameters via the vectors introduced above. The first Stocks' parameter is simply the full field intensity  $I$ , described by (7).

Below, we will present a full field intensity  $I$  via vectors  $\mathbf{C}$  and  $\mathbf{S}$ , or vector  $\mathbf{N}$ , which usually are used in derivations of the depolarized characteristics of the elliptically polarized waves [3, 9–13].

At the same time, as was shown in [3, 9–13], at the close radio traces with shadowing, when the direct wave is absent, we can assume, with a great accuracy, that  $\langle C_i \rangle = \langle S_i \rangle = 0$ ,  $i = 1, 2, 3$ . In this case, the distribution for these six random values can be obtained as follows:

- for a full intensity,  $I = \sum_{i=1}^3 (C_i^2 + S_i^2)$ , as a first Stock's parameter;
- for the intensity of the third component

$$I_3 = C_3^2 + S_3^2 \quad (10)$$

and its phase,  $\psi_3$ .

For convenience, instead of the elliptic parameter  $R$ , we introduce the following parameter

$$\rho = \frac{1 - R^2}{1 + R^2}. \quad (11)$$

The discussion above allows us to state that the differences between the statistical characteristics of the wave,  $\sigma_1^2$  and  $\sigma_2^2$  in the horizontal plane, defined by field components with  $i = 1$  (along the  $x$ -axis) and  $i = 2$  (along the  $y$ -axis), weakly affect distributions of polarized parameters, such as  $R$ ,  $\theta$  and  $\beta$ . Therefore, we can differentiate the vertical direction  $\mathbf{z}$ , defined by  $\sigma_3^2 \equiv \sigma_{\parallel}^2$ , from the horizontal directions, defined by  $\sigma_1^2 \equiv \sigma_{1\perp}^2$  and  $\sigma_2^2 \equiv \sigma_{2\perp}^2$ , which determine the cross-polarized properties in the  $xOy$ -plane.

The relation between the parameter  $p$  and the elliptic coefficient  $R$ , which follows from (11), can be expressed as

$$R = \left( \frac{1 - \rho}{1 + \rho} \right)^{1/2}. \quad (12)$$

Using information either on the parameter  $p$  from (11) or on the elliptic coefficient  $R$  from (12), the shape and the main parameters of the ellipse can be easily predicted.

### Influence of the Built-Up Terrain Characteristics on Wave Depolarization

The 2D multi-parametric stochastic model, without accounting for the buildings' height profile was presented in [3]. Its 3D generalization, accounting for the influence of the buildings' overlay profile, describe the signal intensity distribution in the space domain was presented in [8, 20–22]. We consider the results obtained in [8, 20–22] and

add the fact that the distribution of the signal field strength in the vertical and horizontal plane are uncorrelated, that is:

$$\langle U_{\parallel}(\mathbf{r}_2) U(\mathbf{r}_2) \rangle = 0. \quad (13)$$

We use definitions of the *rms* of signal intensity depolarization with zero-mean Gaussian PDFs in the vertical plane  $\sigma_{\parallel}^2 = \langle U_{\parallel}(r_1) U_{\parallel}^*(r_2) \rangle = \langle I_{inc} \rangle_{\parallel}$  (called the vertical component) and in the horizontal plane  $\sigma_{\perp}^2 = \langle U_{\perp}(r_1) U_{\perp}^*(r_2) \rangle = \langle I_{inc} \rangle_{\perp}$  (called the horizontal component). After some derivations, following [20–22] we get

$$\sigma_{\parallel}^2 = I_0 \frac{\Gamma \lambda \ell_v}{\lambda^2 + [2\pi \ell_v \gamma_0 F(h_R, h_T)]^2} \frac{(h_T - \bar{h})}{d}; \quad (14)$$

$$\sigma_{\perp}^2 = I_0 \frac{\Gamma}{8\pi} \frac{\lambda \ell_h}{\lambda^2 + [2\pi \ell_h \langle L \rangle \gamma_0]^2}. \quad (15)$$

Here  $I_0$  is the intensity of the transmitted signal;  $\Gamma$  is the absolute value of its deterministic part;  $\ell_v$  and  $\ell_h$  are the correlation scales of the diffuse reflection coefficients in the vertical and horizontal plane, respectively;  $F(h_R, h_T)$  is the profile functions describing building heights distribution along the radio path between Rx (with the height  $h_R$ ) and Tx (with the height  $h_T$ ) in the vertical plane;  $\bar{h}$  is the average buildings' height, and all other parameters are already defined in previous sections  $L \equiv \langle L \rangle$  is the average length of building;  $\gamma_0 = 2LV/\pi$  is the 1D density of the buildings contours,  $V$  is the building density per [in  $\text{km}^2$ ].

By investigating numerous urban overlay profiles, it was shown in [20–22] that the more realistic buildings' profile occur in urban scenarios, where the number of tall buildings is roughly equal to the number of small buildings. In such scenarios, usually occurring in the urban environment, the profile function can be simplified as in [22]. For these built-up scenarios equation (14) can be written as

$$\sigma_{\parallel}^2 = I_0 \frac{\Gamma \lambda \ell_v}{\lambda^2 + [2\pi \ell_v \gamma_0 (\bar{h} - h_R)]^2} \frac{(h_T - \bar{h})}{d}. \quad (16)$$

We will analyze the ratio  $\sigma_{\parallel}^2 \equiv \sigma_{\perp}^2$  for various densities of buildings, typical for many small towns and large cities. From expressions (14)–(16), this ratio depends mostly on the density of buildings,  $\gamma_0$ , and on the elevations of both terminal antennas,  $h_R$  and  $h_T$ , with respect to the average buildings' height, that is

$$\frac{\sigma_{\parallel}^2}{\sigma_{\perp}^2} = 8\pi \frac{\ell_v}{\ell_h} \frac{1 + \frac{[2\pi \ell_h \gamma_0 \langle L \rangle]^2}{\lambda^2}}{1 + \frac{(2\pi \ell_v \gamma_0 (\bar{h} - h_R))^2}{\lambda^2}} \frac{h_T - \bar{h}}{d}. \quad (17)$$

■ **Table 1.** The model parameters for built-up areas

Area type	$h_R$ , m	$h_T$ , m	$d$ , km	$L$ , m	$l_h, l_v$ , m	$V, \frac{\text{buildings}}{\text{km}^2}$	$\Gamma$
Rural	2–3	20–50	0.5, 1, 2, 5	10–15	1–2	10–20	0.4 (wood)
Mixed Residential	3–5	20–50	0.5, 1, 2, 5	20–40	1–2	30–40	0.7 (stone)
Sub Urban	3–10	15–30	0.2, 0.5, 1, 2	50–60	2–3	50–60	0.7 (glass)
Urban	2–10	40–60	0.2, 0.5, 1, 2	80–100	3–5	70–90	0.8 (steel)

For high buildings density located at the ground surface and a “smooth” building profile in the vertical plane (i.e., when  $(\bar{h} - h_R)$  and  $(h_T - \bar{h})$  are close), for distances beyond 100 m, and for  $(l_v/l_h) \approx 1$ , we get  $\sigma_{\parallel}^2 / \sigma_{\perp}^2 < 1$ . In this case, the degree of polarization discrimination caused by the multi-ray phenomena in the horizontal plane, that is, by multiple scattering, diffraction and reflection, becomes stronger with respect to that in the vertical plane. Conversely, for the “sharp shaped” building profile and a small buildings density located at the ground surface for similar other conditions, we get that  $\sigma_{\parallel}^2 / \sigma_{\perp}^2 > 1$ .

Finally, when the character of signal energy due to multipath phenomena becomes “random” and similar both in the horizontal and vertical plane (large city scenario), we get  $\sigma_{\parallel}^2 / \sigma_{\perp}^2 \approx 1$ . This qualitative analysis allows us now to investigate the parameters of the polarization ellipse of the incident radio wave for various scenarios occurring in the built-up terrestrial environment with different ratios of  $\sigma_{\parallel}^2 / \sigma_{\perp}^2$ .

## Numerical Simulation and Results

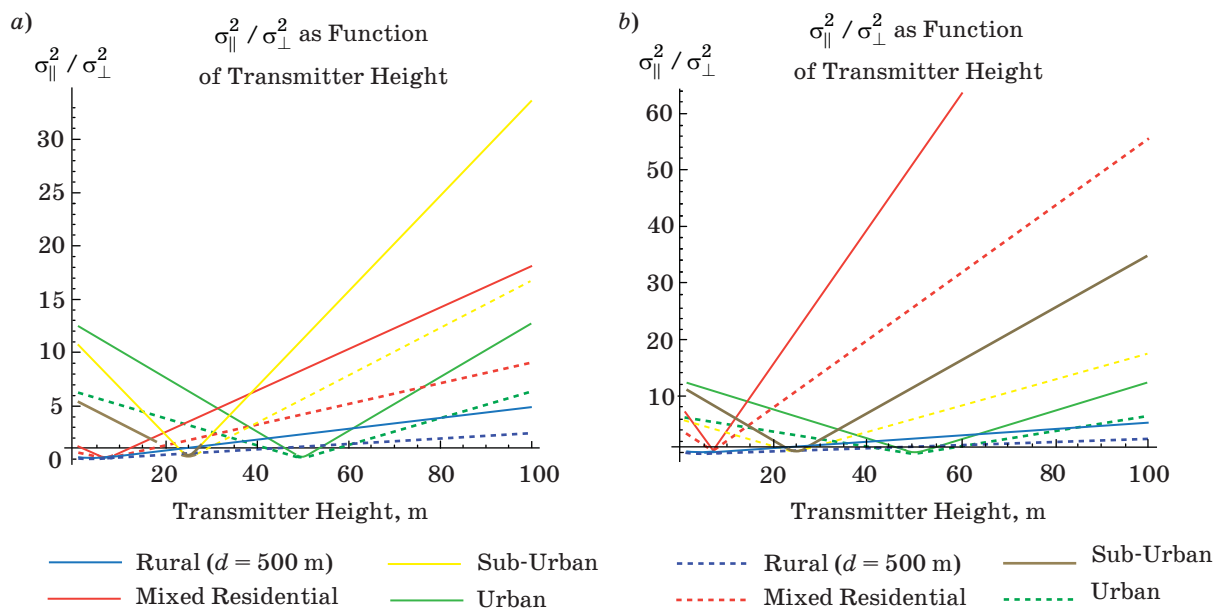
### Areas Selection and their Topographic Features and Parameters

We divided the areas under study into four different types: Rural, Mixed Residential, Sub-Urban, and Urban. This division yields large differences between the various built-up area characteristics. In order to evaluate every area parameter, we used data presented in [19–26, 32] for various rural, mixed residential and urban areas, and finally took the average of each parameter as presented in Tab. 1, estimating the ranges of values of their variations.

### Analysis of the Ratio $\sigma_{\parallel}^2 / \sigma_{\perp}^2$ of the Polarization Ellipse

*The  $\sigma_{\parallel}^2 / \sigma_{\perp}^2$  ratio vs. the BS height*

The following graphs represent the ratio between the vertical component and horizontal component, as a function of the BS height, for distances of 500 m and 1000 m between the Rx and Tx antennas operating with the frequency of 1.8 GHz (Fig. 1, a) and



■ **Fig. 1.** The  $\sigma_{\parallel}^2 / \sigma_{\perp}^2$  ratio vs. BS height for the distance of 500 m (solid curves) and 1000 m (dotted curves), with operating frequency of  $f = 1.8$  GHz (a) and  $f = 5.7$  GHz (b)

of 5.7 GHz (Fig. 1, b). The location of the horizontal axis represents the ratio  $\sigma_{\parallel}^2 / \sigma_{\perp}^2 = 1$ , which means that when the ratio is above the horizontal axis, the vertical component is smaller than the horizontal component. The situation when the ratio is below the horizontal axis indicates cases when the vertical component is bigger than the horizontal component.

From Fig. 1, for every type of terrain, the minimal ratio is achieved when the BS antenna is located at the level of the average height of buildings and when the ratio becomes smaller than the unit. In fact, when the BS antenna is located at the level of the average building height, the horizontal and vertical components of the elliptical polarized field are roughly the same. With changes of the BS antenna height (to be less or more than the average height of the buildings' profile), the vertical component is increased, due to a decrease of signal losses caused by the multipath (stochastic) interference, and therefore, the ratio is also increased.

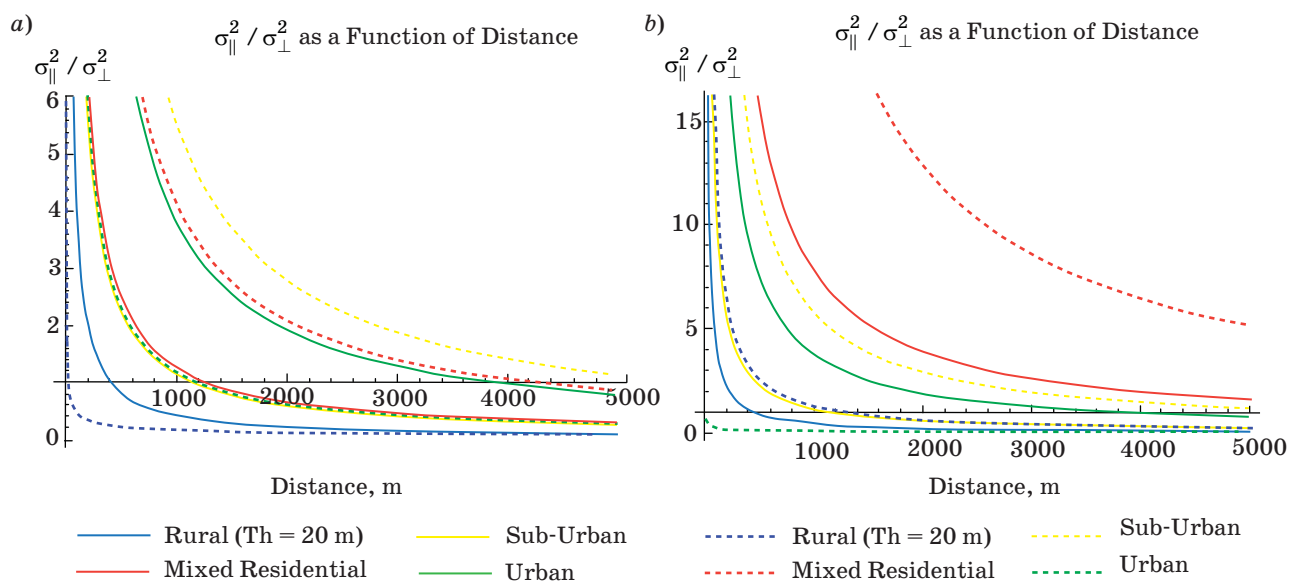
Next, for every type of terrain with an increase in the Tx-Rx distance, the ratio  $\sigma_{\parallel}^2 / \sigma_{\perp}^2$  decreases due to stronger signal losses in the vertical plane with respect to those in the horizontal plane, and as the result, with increase of Rx-Tx distance the ratio also decreases. Moreover, from the presented illustrations, it is clear that for rural areas the ratio  $\sigma_{\parallel}^2 / \sigma_{\perp}^2$  is smaller than 1, because in this terrain, the BS height is low enough and due to stronger sporadic interference caused by multipath effects in the horizontal plane with respect to that in the vertical plane. As for the urban areas, it is seen that the ratio becomes larger than unit because the transmitter height is much higher than the average height of surrounding buildings. Here, conversely, the horizontal

component is smaller than the vertical component, and the building density becomes a more significant parameter of the multipath in the vertical plane due to multiple diffraction from buildings roofs in the vertical plane, with respect to multiple scattering from buildings' walls in the horizontal plane.

$\sigma_{\parallel}^2 / \sigma_{\perp}^2$  vs. the distance between BS and MS antennas

Figure 2 represents the ratio between the vertical and horizontal components as a function of the distance between the BS and MS antennas for the height of the BS equals 20 m and 50 m for frequencies of 1.8 GHz (see Fig. 2, a) and 5.7 GHz (see Fig. 2, b). As before, the location of the horizontal axis represents the ratio  $\sigma_{\parallel}^2 / \sigma_{\perp}^2$  (that is, equals 1). This means that the vertical component is smaller than the horizontal component, when its value is below this axis, and is bigger, when it is above this axis.

Again, for rural areas, all curves lie along the horizontal axis, that is,  $\sigma_{\parallel}^2 / \sigma_{\perp}^2$  is almost always less than 1, which means that the horizontal component is bigger than the vertical component compared with built-up areas, where most of the curves exceeded 1. With the decrease in transmitter height (limiting to the receiver height),  $\sigma_{\parallel}^2 / \sigma_{\perp}^2 < 1$ . This is evident since the vertical component becomes smaller than the horizontal component, due to much stronger interference in the vertical plane. Moreover, when the transmitter achieves the average height of the building profile, lower line-of-sight condition is observed in the vertical plane causing stronger interference and the corresponding radio signal loss. When the distance between the receiver and transmitter is short, the observed interference becomes weaker



■ Fig. 2. The  $\sigma_{\parallel}^2 / \sigma_{\perp}^2$  ratio vs. the distance between BS and MS for the BS antenna height of 20 m (solid curves) and 50 m (dotted curves), the frequency of  $f = 1.8$  GHz (a) and  $f = 5.7$  GHz (b)

resulting in an increase of the vertical component of the elliptically polarized wave, and the ratio  $\sigma_{\parallel}^2 / \sigma_{\perp}^2$  increases. As the distance between the transmitter and receiver is increased, the ratio  $\sigma_{\parallel}^2 / \sigma_{\perp}^2$  decreases due to the increase of the sporadic interference phenomena caused by the strong multipath effect in the vertical plane (called the randomization of the vertical component of the elliptically polarized wave).

**Analysis of the Loss Characteristics of the Vertical and Horizontal Components**

We analyze each component of the elliptically polarized radio wave and present below the loss [in dB] for both components separately vs. buildings' density and additionally vs. the distance between Rx and Tx for only vertical component of the field energy. Computations were carried out for each type of the terrain with its specific parameters shown in Tab. 1 and for the operating carrier frequency of the BS of 2.4 GHz.

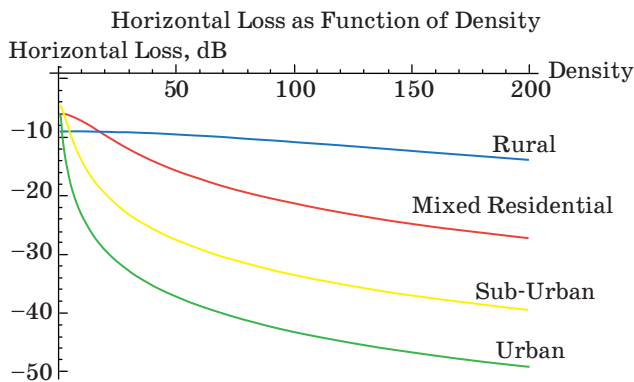
*Horizontal component of the total elliptically polarized field*

Results of computations are shown in Fig. 3. One can see that in rural areas the loss is smaller than in other area types (the difference is roughly ~10 dB) mainly due to signal power loss. In urban areas the depolarization loss increases significantly as long as density of buildings surrounding both terminal antennas, Rx and Tx, increases (averagely on ~40 dB). It is seen that with an increase of buildings' density surrounding the Rx and Tx antennas, the interference loss has tendency to increase drastically due to multipath phenomena occurring in the horizontal plane.

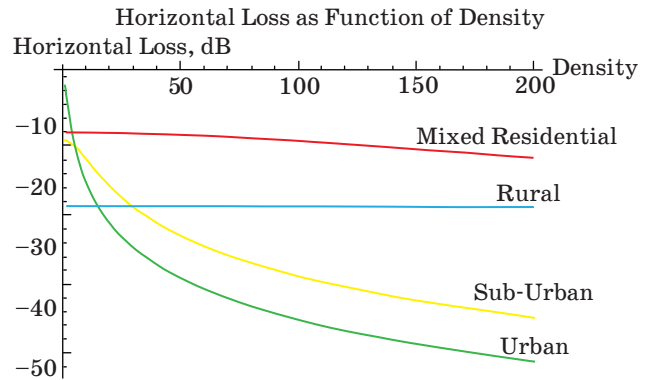
*Vertical component of the total field vs. buildings' density*

The corresponding results of computations are shown in Fig. 4.

It is seen from the presented illustrations that when the distance between the transmitter (BS)



■ Fig. 3. Loss of the horizontal component vs. buildings density for all four typical land environments



■ Fig. 4. Vertical component of the total elliptical wave field vs. buildings density for all four typical land environments

and receiver (MS) increases the loss in the vertical component is apparent. In sub-urban and mixed-residential areas the distance between the transmitter and the receiver may be increased, in order to cover more ground, because the loss is relatively reasonable. On the contrary, in purely urban areas, one cannot increase the distance between the transmitter and the receiver since the loss is significant: in such areas we need to bring the transmitter and the receiver close to each other, in order to decrease signal loss in accordance with area constraints.

**Depolarization Angle as a Function of Transmitter Height**

The angle of depolarization  $\gamma$  can be defined as (usually it is taken to be positive [8–17])

$$\gamma = \left| \sin^{-1} \frac{\sqrt{\sigma_{\parallel}^2}}{\sqrt{\sigma_{total}^2}} \right| = \left| \sin^{-1} \frac{\sqrt{\sigma_{\parallel}^2}}{\sqrt{\sigma_{\perp}^2 + \sigma_{\parallel}^2}} \right|. \quad (18)$$

This parameter, usually called antenna cross-polarization discrimination, plays an important role in determining the propagation channel or the corresponding antenna performance [8].  $\gamma$  determines the corresponding polarization loss factor (PLF), which is used as a figure of merit to measure the degree of polarization mismatch. The PLF is defined through the angle of depolarization as [8]

$$PLF = |\cos \gamma|^2. \quad (19)$$

To investigate the ratio  $\sigma_{\parallel}^2 / \sigma_{\perp}^2$ , the angle of depolarization, and PLF, we examined for all four known types using the following two scenarios: a) when the transmitter antenna is higher than the average height of the buildings height and quasi-loss scenario; b) when the transmitter is at the level of the average buildings height.

As it follows from Tab. 2, in urban and sub-urban areas the angle of depolarization increases dramati-

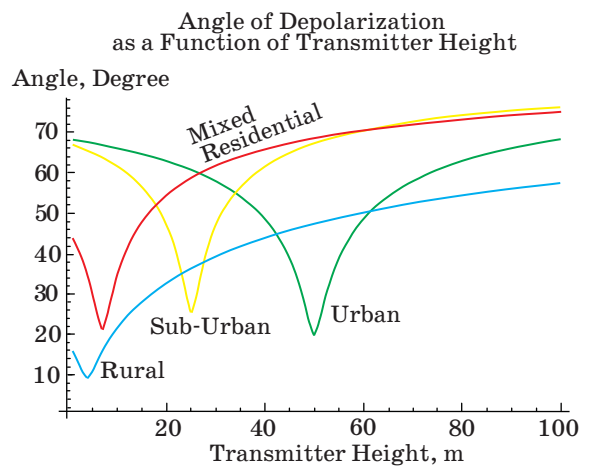
■ **Table 2.** Results for scenarios a and b, with 2.4 GHz frequency

Area	Scenario a $h_t =  \bar{h} - h_r  + h_r$			Scenario b $h_t = \bar{h}$		
	Angle of Depolarization	PLF	$\sigma_{\parallel}^2 / \sigma_{\perp}^2$	Angle of Depolarization	PLF	$\sigma_{\parallel}^2 / \sigma_{\perp}^2$
Rural	8.7	0.022	0.023	6.1	0.011	0.011
Mixed Residential	33.5	0.304	0.439	16.4	0.079	0.08
Sub-Urban	60.0	0.75	3.05	19.15	0.107	0.12
Urban	70.6	0.889	8.14	18.77	0.103	0.11

cally, as well as the ratio  $\sigma_{\parallel}^2 / \sigma_{\perp}^2$  and PLF compared to the rural area, where the parameters of the polarization discrimination are negligible. It is evident that in urban and sub-urban environments, due to multiple diffractions from building roofs and corners, the vertical component of the total field intensity variations  $\sigma_{\perp}^2$ , exceeds the horizontal component  $\sigma_{\parallel}^2$ .

At the same time, the PLF can achieve small values ( $10\log_{10}(PLF) \in [-3, -1]$  dB) in these two area types, since it fully determined by deterministic multi-diffraction processes in the vertical plane, and the effects of random multi-scattering process occurring in the horizontal and vertical planes can be mitigated. As for rural and mixed-residential areas, here the angle of polarization mismatch is relatively small, the PLF can achieve higher magnitudes of  $10\log_{10}(PLF) \in [-16, -19]$  dB and the horizontal component becomes to be prevailed, indicating the importance of the multipath phenomena due to multiple scattering from obstructions located in the horizontal plane.

Results for scenario b, where the transmitter antenna is located at the rooftops level, are also given in Tab. 2. Here we observe the same tendency of an increase in the angle of depolarization, by approaching of sub-urban and urban areas from the rural areas. But this increase in the depolarization angle is too “smooth” compared to the one described above with described above following results shown for scenario a. The corresponding PLF is also relatively smaller compared to the situation described in case a. This also can be explained by the increasing of the role of the horizontal component with respect to the vertical component. This means that in the horizontal plane random processes of multipath become predominant, and the PLF parameter can achieve in urban and suburban environments magnitudes of  $-10$  dB, whereas in mixed residential and rural areas, its magnitude increases drastically achieving even  $-20$  dB, indicating role of random multi-path processes, such as multiple scattering from obstructions, in total wave field depolarization. Simultaneously, a decrease in angle of angle depolarization was accompanied by the increase of the ratio  $\sigma_{\parallel}^2 / \sigma_{\perp}^2$ , and decrease in the PLF [being negative in dB].



■ **Fig. 5.** The angle of depolarization vs. the height of the transmitter for four typical land built-up scenarios

Figure 5 shows the angle of depolarization as a function of transmitter height for a distance of 1000 m for the carrier frequency of 2.4 GHz. The illustrated graphs for all four studied built-up areas, parameters of which are introduced in Tab. 1, show the same tendency as the previous figures, that is, when transmitter height in closer to the level of the average building’s height, the angle of depolarization limits to its minimal value. With the increase in the transmitter height with respect to the buildings roofs, defined by the average height  $\bar{h}$ , the angle of depolarization increases significantly.

Moreover, the corresponding interference picture (e.g., oscillations of the field intensity with height) is clearly seen from Fig. 5 approaching the environment, from rural and mixed residential (without oscillations) to sub-urban and urban (with essential oscillations).

### Summary and Conclusions

In order to predict the influence of depolarization on propagation of the elliptically-polarized radio wave, it is necessary to obtain information on the main characteristics and parameters of the terrain.

In fact, each of the discussed terrain types acts like a communication channel that “reacts” differently on the input propagation parameters, that is, on the propagation environment within each channel: urban, sub-urban, mixed-residential and rural.

The channel “reaction” depends on different terrain factors: antenna location and elevation with respect to buildings’ heights, obstructions’ characteristics (e.g., the permittivity of the material – stone, wood, steel, glass, etc.), buildings’ density, distance between the transmitter and the receiver, degree of roughness of the walls, buildings width or length, terrain topography, and so on.

The formulas that describe the intensity distribution of the elliptically-polarized radio wave inside the ellipse, which until recently were not presented in the literature, were derived based on main formulas of signal intensity distribution in space domain based on the multi-parametric stochastic theoretical framework that describes radio propagation in various terrain environments.

The simple “engineering” formulas for radio wave intensity deviations in the vertical and horizontal planes of the ellipse, the corresponding angle of depolarization as function of its vertical and horizontal components, and the PLF were derived based on the proposed stochastic approach.

The corresponding 3D numerical code was performed for analysis of the corresponding formulas for various terrain scenarios, urban, sub-urban, mixed-residential, and rural, depending on the built-up terrain features.

Depolarization effects and polarization losses were analyzed for four types of environment: rural, mixed-residential, sub-urban, and urban.

The obtained results allow us to state additionally that:

1. In rural and mixed residential areas the vertical component of the elliptically polarized radio wave is not changed significantly (e.g., has small depolarization loss), and the angle of depolarization is too small with respect to that obtained in urban and sub-urban areas. This allows us to suggest the

increase of the range between transmitting (Tx) and receiving (Rx) antenna in such areas.

2. In urban and sub-urban areas the wave intensity loss is significant both in the vertical and the horizontal planes of the elliptically-polarized wave, caused by the random interference of its multipath components due to multi-scattering, multi-diffraction and multi-reflection phenomena from obstructions surrounding both terminal antennas.

3. As expected, the angle of depolarization is larger for urban channels with the corresponding increase of the PLF. This effect strongly depends on the height of the transmitter antenna (receiver antenna was always lower than buildings’ roofs) with respect to average buildings’ height. Thus, the angle of depolarization decreases with decrease of transmitter antenna height, and vice versa — with increase of transmitter antenna height.

4. The ratio between vertical and horizontal components of the elliptically-polarized wave increases with transfer of the channel from rural to urban scenarios. This means that the effect of depolarization becomes more significant in the more dense built-up environments.

5. Increase of depolarization of the even elliptically-polarized radio wave, passing through the sub-urban and urban channels, yields the increase the randomization of the wave intensity both in the vertical and horizontal plane leading to changes in shape of the ellipse and its rotation in a large angle (see Tab. 2).

6. Additionally, increase of depolarization loss and the angle of depolarization yield the decrease of signal power and require additional signal amplification at the receiver.

7. Knowledge of the “reaction” of each individual channel (urban, sub-urban, mixed-residential and rural) on signal depolarization allows to give for each designer of wireless communication links a powerful tool for predicting a priori the influence of the built-up channel “response” on the depolarization phenomena accounting for each specific scenario occurring at the built-up scene.

## References

1. Stutzman W. L., and G. A. Thiele. *Antenna Theory and Design*. New York, John Wiley & Sons, 1981. 598 p.
2. Kraus J. D. *Antennas*. 2nd ed. New York, McGraw-Hill, 1988. 892 p.
3. Ponamarev G. A., Kulikov A. N., and Tel’pukhovskiy E. D. *Propagation of Ultra-Short Waves in Urban Environments*. Tomsk, Rasko Publ., 1991. 222 p. (In Russian).
4. Balanis C. A. *Antenna Theory: Analysis and Design*. 2nd ed. New York, John Wiley & Sons, 1997. 941 p.
5. Drabowitch S., Papiernik A., Griffiths H., Encinas J., and Smith B. L. *Modern Antennas*. London, Chapman & Hall, 1998. 611 p.
6. Kraus J. D., and Marhefka R. *Antennas*. New York, McGraw-Hill, 2001. 547 p.
7. Chryssomallis C., and Christodoulou Ch. *Antenna Radiation Patterns*. In: *John and Wiley Encyclopedia of Electrical and Electronics Engineering*, 2001, ch. 3, pp. 164–175.
8. Blaunstein N., and Christodoulou C. *Radio Propagation and Adaptive Antennas for Wireless Communication Links: Terrestrial, Atmospheric and Ionospheric*. New Jersey, Wiley and Sons-InterScience, 2008. 614 p.

9. **Morgan M., and Evans V.** Synthesis and Analysis of Polarized Ellipses. In: *Antennas of Elliptic Polarization*. New York, John Wiley & Sons, 1961. 385 p.
10. **Kanare'kin D. B., Pavlov N. F., and Potekhin V. A.** *Polarization of Radiolocation Signals*. Moscow, Sovetskoe radio Publ., 1966. 440 p. (In Russian).
11. **Gusev K. G., Filatov A. D., and Sopolev A. P.** *Polarization Modulation*. Moscow, Sovetskoe radio Publ., 1974. 286 p. (In Russian).
12. **Lee W. C., and Brandt R. H.** The Elevation Angle of Mobile Radio Signal Arrival. *IEEE Trans. Commun.* 1973, vol. 21, no. 11, pp. 1194–1197.
13. **Bitler Y. S.** A Two-Channel Vertically Spaced UHF Diversity Antenna System. *Proc. of Microwave Mobile Radio Symp.*, Colorado, 1973, pp. 13–15.
14. **Kozono S., Tsuruhara T., and Sakamoto M.** Base Station Polarization Diversity Reception for Mobile Radio. *IEEE Trans. on Vehicular Technology*, 1984, vol. 33, no. 4, pp. 301–306.
15. **Vaughan R. G., and Andersen J. B.** Antenna Diversity in Mobile Communications. *IEEE Trans. on Vehicular Technology*, 1987, vol. 36, no. 4, pp. 149–172.
16. **Vaughan R. G.** Polarization Diversity in Mobile Communications. *IEEE Trans. on Vehicular Technology*, 1990, vol. 39, no. 3, pp. 177–186.
17. **Lemieux J-F., El-Tanany M. S., and Hafez H. M.** Experimental Evaluation of Space/Frequency/Polarization Diversity in the indoor Wireless Channel. *IEEE Trans. on Vehicular Technology*, 1991, vol. 40, no. 3, pp. 189–198.
18. **Turkmani A. M. D., Arowojolu A. A., Jefford P. A., and Kellett C. J.** An Experimental Evaluation of the Performance of Two-Branch Space and Polarization Diversity Schemes at 1800 MHz. *IEEE Trans. on Vehicular Technology*, 1995, vol. 44, no. 2, pp. 318–326.
19. **Bertoni H. L.** *Radio Propagation for Modern Wireless Systems*. New Jersey, Prentice Hall PTR, Inc., 2000. 258 p.
20. **Blaunstein N.** Prediction of Cellular Characteristics for Various Urban Environments. *IEEE Antennas and Propagat. Magazine*, 1999, vol. 41, no. 6, pp. 135–145.
21. **Blaunstein N., Giladi R., Levin M.** Unified Approach to Predict of Loss Characteristics in the Urban Microcellular Environments with Rectangular Grid-plan Streets. *Radio Science*, vol. 34, no. 5, 1999, pp. 1085–1102.
22. **Blaunstein N., Censor D., Katz D., Freedman A., and Matityahu I.** Radio Propagation in Rural Residential Areas with Vegetation. *J. Electromagnetic Waves and Applications*, 2002, vol. 17, no. 7, pp. 1039–1041.
23. **Blaunstein N.** Distribution of Angle-of-Arrival and Delay from Array of Buildings Placed on Rough Terrain for Various Elevations of Base Station Antenna. *Journal of Communications and Networks*, 2000, vol. 2, no. 4, pp. 305–316.
24. **Blaunstein N., Katz D., Censor D., Freedman A., Matityahu I., and Gur-Arie I.** Prediction of Loss Characteristics in Built-up Areas with Various Buildings Overlay Profiles. *IEEE Anten. Propagat. Magazine*, 2001, vol. 43, no. 6, pp. 181–191.
25. **Blaunstein N., Toulch M., Bonek E., Christodoulou Ch., et al.** Azimuth, Elevation and Time Delay Distribution in Urban Wireless Communication Channels. *Journal of Antennas and Propagation Magazine*, 2006, vol. 48, no. 2, pp. 112–126.
26. **Blaunstein N., Toulch M., Laurila J., Bonek E., et al.** Signal Power Distribution in the Azimuth, elevation and Time Delay Domains in Urban Environments for Various Elevations of Base Station Antenna. *IEEE Trans. Antennas and Propagation*, 2006, vol. 54, no. 10, pp. 2902–2916.
27. **Lempianen J., Laiho-Steffens J. K., and Walker A. F.** Experimental Results of Cross Polarization Discrimination and Signal Correlation Values for a Polarization Diversity Scheme. *Proc. of 47th IEEE Vehicular Technology Conf.*, 1997, pp. 1498–1502.
28. **El-Sallabi H. M., and Tervonen J.** Polarization Dependence of Multipath Propagation Characteristics in Line of Sight Microcellular Channels. *Proc. of 12th Int. Conf. on Wireless Communication (Wireless 2000)*, Canada.
29. **El-Sallabi H. M.** Polarization Consideration in Characterizing Radio Wave Propagation in Urban Microcellular Channels. *Proc. of 51st Vehicular Technology Conf.*, Greece, 2001, pp. 411–415.
30. **Shapira J., and Miller S.** A Novel Polarization Smart Antenna. *Proc. of 51st Vehicular Technology Conf.*, Greece, 2001, pp. 253–257.
31. **Shapira J., and Miller S.** Transmission Considerations and Polarization Smart Antennas. *Proc. of 51st Vehicular Technology Conf.*, Greece, 2001, pp. 258–262.
32. **Bertoni H. L., and Walfisch J.** A Theoretical Model of UHF Propagation in Urban Environment. *IEEE Trans. on Antennas and Propagation*, 1988, vol. 36, no. 12, pp. 1788–1796.